6300 *Macromolecules* **2009**, *42*, 6300–6309
DOI: 10.1021/ma9007412

Macromolecules
ARTICLE

New Numerical Implementation of Self-Consistent Field Theory for Semiflexible Polymers

Wendi Song,[†] Ping Tang,*[,†] Hongdong Zhang,[†] Yuliang Yang,*[,†] and An-Chang Shi[‡]

[†]*Key Laboratory of Molecular Engineering of Polymer, Ministry of Education, and Department of Macromolecular Science, Fudan University, Shanghai 200433, China, and* [‡]*Department of Physics and Astronomy, McMaster University, Hamilton L8S 4M1, Canada*

Received April 6, 2009; Revised Manuscript Received June 15, 2009

ABSTRACT: A new real-space numerical implementation of the self-consistent field theory for semiflexible polymers is developed. Specifically, a finite volume algorithm on a unit sphere with an icosahedron triangular mesh is employed to describe the orientation degree of freedom of the wormlike chains. The validity of the new method is analyzed by comparing with results from the spectral method. As a concrete example, the new numerical method is applied to the self-assembly of rod−coil diblock copolymers within the framework of Onsager excluded-volume interaction. A variety of liquid crystalline phases such as disordered isotropic, nematic, and smectic phases have been obtained. In particular, the new method provides a particularly convenient method for studying the smectic-C phase. A phase diagram is constructed for the rod−coil diblock copolymers, which is in agreement with previous theoretical and experimental results.

I. Introduction

One of the most successful theories for polymeric systems is the self-consistent field theory (SCFT), which transforms the statistical mechanics of many polymers into a field theory.[1] The essence of SCFT is that the statistics of polymer chains is described by a propagator, which is the probability of finding a particular chain segment at a particular state. For the simplest case of Gaussian chains, the state of a segment is completely specified by its position. In this case, the propagator satisfies a modified diffusion equation. In the past decades, a variety of efficient numerical methods have been developed to solve the SCFT equations for flexible (Gaussian) polymers.[2−4] For the case of semiflexible or wormlike polymers, the state of a segment is specified by its position and orientation. In this case, the propagator satisfies a diffusion-like equation in the 5D space composed of a 3D position space and a 2D orientation space. Finding solutions of this 5D diffusion equation presents a challenge to the polymer physics community. A number of numerical methods have been proposed to address this challenge.[5−8] Most of these previous studies are either based on a spectral method or with further assumptions about the chain rigidity. Therefore new numerical methods for the solution of semiflexible polymers are desirable.

From an application perspective, liquid-crystalline block copolymers, with a rigidity originated from π-conjugation (semiconducting polymers), helical secondary structures (biomolecules), or aromatic groups (aramide and aromatic polyester high-performance resins), attract increasing attention because these polymers are essential ingredients in a wide range of applications such as organic electronics, biological molecules, and superstrong engineering resins.[9] However, when rigidity is introduced into block copolymer chains, the phase behavior becomes much more complex because orientation order will play an important role in the different phases. The coupling of microphase separation and orientation ordering leads to a very rich array of liquid-crystalline phases such as nematic and layered smectic structures that are distinct from the classical coil−coil diblock copolymers. Experimentally, it has been observed that both rod−coil diblock copolymer solution and melt exhibit a number of intriguing phases including wavy lamellae,[10] zigzags,[10] arrowheads,[10] straight lamellae,[11] perforated lamellae,[12−14] hexagonal stripes,[11,15,16] pucks,[12,15−17] spheres,[18,19] cylindrical,[20−22] and bicontinuous cubic[11,23,24] morphologies. In addition, phase diagrams of rod−coil diblock copolymers have been constructed from experiments.[25−27] A generic feature is that the liquid crystalline interactions stabilize planar interfaces, leading to a larger lamellar region in the phase space when compared with coil−coil diblock copolymers. The self-assembly of rod−coil diblock copolymer thin films[28,29] presents additional challenges because of the confinement of the surfaces. The richness of the self-assembly of rod−coil diblock copolymers[9,30] has the potential to provide an elegant path to produce nanoscale structure, similar to what has been done with coil−coil block copolymers. To achieve this goal, it is desirable to obtain theoretical understanding of the phase behavior and self-assembly mechanism of rod−coil block copolymers.

In contrast with the vast body of theoretical studies of flexible diblock copolymers, theoretical research of the self-assembly of diblock copolymers with some degree of rigidity is limited. For rodlike block copolymers, many factors including chain stretching, isotropic Flory−Huggins interaction, and the topology and orientation interactions of the rod blocks will influence the free energy and equilibrium structures. The microphase separation of rod−coil diblock copolymers was analyzed by Semenov and Vasilenko[31] in the strong segregation regime and with the assumption that the rods are strictly aligned along the lamellae normal. Subsequently, Semenov[32] and Halperin[33] used analytical free energy calculations and scaling relationships to understand the liquid crystal behavior and predicted the transitions between nematic, smectic-A, and smectic-C phases. Monolayer and bilayer lamellae were obtained according to segregation strength and the surface free energy penalty to the entropic stretching of

*Corresponding authors. E-mail: pingtang@fudan.edu.cn (P.T.); yuliangyang@fudan.edu.cn (Y.Y.).

 Published on Web 07/24/2009

the flexible block. Later, Williams and Fredrickson[34] extended these analytical theories to examine the "hockey puck" micelles for coil-rich rod−coil diblock copolymers, assuming that the rods were packed axially into cylinders. In another study, Holeyst and Schick[35] studied the order−parameter correlation functions of rod−coil diblock copolymers. Their theory provided some general features of the phase diagram and found that the appearance of the nematic phase was the direct consequence of the anisotropic interactions. Reenders and ten Brinke[36] derived a fourth-order free energy expansion in both composition and orientation order parameters. These authors obtained microphase-separated structures such as hexagonal, BBC, and spherical without orientational order in the coil-rich region, which was similar to those of coil−coil self-assembly. For high volume fractions of the rod block, the system exhibited typical liquid-crystalline behaviors with an isotropic-to-nematic-to-smectic-C transition. It should be noticed that these theoretical models are restricted to the weak segregation limit or the strong segregation limit. However, most experiments of rod−coil diblock copolymers are carried out in the intermediate region.

For block copolymers in the intermediate segregation region, neither strong segregation theory nor weak segregation theory are applicable. In this case, the most efficient method is to solve the SCFT equations numerically. Numerical implementation of SCFT of flexible Gaussian chains has been well developed. It provides a powerful tool for the study of the self-assembly of complex block copolymer systems, including multiblock copolymers with different chain architectures,[37,38] the aggregation behaviors of copolymers in solution,[39] polymers confined under special geometric conditions,[40] and block copolymer−nanoparticle blends.[41] However, the application of numerical SCFT studies of rod−coil diblock copolymers is still limited. Muller and Schick[42] studied ordered phases of rod−coil diblock copolymers by a partial numerical evaluation of the single chain partition function instead of numerically calculating diffusion equation for the chain propagator. Their method was applied to the weak segregation limit, and the anisotropic interactions between the rods were ignored. Matsen and Barrett[43] performed the SCFT calculation to investigate the liquid-crystal behavior of the rod−coil system using the Semenov−Vasilenko model[31] and assuming that all rods are strictly aligned along the same direction. Furthermore, the bending configuration energy between rigid segments and **u**-dependence of the chain propagator is ignored. In a later study, Pryamitsyn and Ganesan[44] performed similar SCFT calculations with a Maier−Saupe interaction between the rods. They have explored the phase diagrams including both 1D and 2D spatial variation of the densities, focusing on nonlamellar phases such as puck and broken lamellar phases at high coil volume fractions in their 2D calculations. However, in their work, the rod blocks were treated as completely rigid, thus ignoring the bending penalty. It is expected that this treatment would become inaccurate at high coil volume fractions. Some other theoretical models did not consider liquid-crystal interactions between the rods. For instance, Chen et al.[45] as well as Li and Gersappe[46] performed lattice-based SCFT simulations. Their models ignored anisotropic aligning interactions between the rods. The asymmetric phase diagram was found as a result of the presence of the rigid blocks, different from that of coil−coil diblock copolymers. In addition to these theoretical studies, simulations such as dynamic SCFT,[47,48] Brownian dynamics,[49] and Monte Carlo simulations[50,51] were performed to study the phase behavior of rod−coil system.

The difficulty of treating polymer chains with rigidity is to incorporate the orientation degree of freedom of the chain segments in the theory. A generic model to describe chain rigidity is the wormlike chain model. In the wormlike chain model, an orientation variable, in the form of a unit vector, **u**, is used to describe the segment orientation. As a result, the chain propagator $q(\mathbf{r},\mathbf{u},t)$ has two additional internal coordinates to describe the orientation dependence of the function, resulting in increased calculation costs and difficulties. Because of these difficulties, the numerical implementation of the SCFT study based on the wormlike chain model is quite limited. Masten[5] examined periodical lamellar structures of semiflexible diblock copolymers by implementation of the SCFT with wormlike chain model. A fully spectral algorithm is used to numerically solve the chain propagator $q(\mathbf{r},\mathbf{u},t)$, where basis functions that are orthonormal and eigenfunctions of $\nabla_{\mathbf{r}}$ and $\nabla^2_{\mathbf{u}}$ were used to describe the space dependence and orientation dependence. The number of basis functions is determined by the convergence of results, but the orientational interaction is not considered in his model system. Netz and Schick[52] simulated the phase behavior of semiflexible diblock copolymers using the SCFT with the wormlike chain model. Similar to the method of Matsen, the SCFT equations were numerically solved by expanding all functions related to **r** and **u** in a complete, orthonormal set of eigenfunctions of the Laplacian on the unit sphere $\nabla^2_{\mathbf{u}}$ and on the spatial space $\nabla_{\mathbf{r}}$. The difference is that in the work of Matsen the anisotropic orientational interactions between the rigid blocks is ignored, whereas Netz and Schick used the Maier−Saupe models to describe the anisotropic orientational interactions. In a series of recent studies, Sullivan et al.[6,53,54] adopted a hybrid approach to numerically solve the diffusion equation of the propagator for wormlike chains. Their numerical method involved expanding the orientation dependence in spherical harmonics and applying finite differences in both **r** and t. Although the extension of this approach to describe the **u** dependence in 3D is straightforward conceptually, the computation is exceedingly costly in the general cases of $m \neq 0$ in the spherical harmonics $Y_{l,m}(\mathbf{u})$. Because of this computational difficulty, current application of the hybrid spectral method has been restricted to the ordered phases with axial symmetries, such as the nematic and smectic-A phases. The axial symmetry ensures that $m = 0$ in the spherical harmonics $Y_{l,m}(\mathbf{u})$ so that the computation demand is greatly reduced. On the other hand, ordered phases with broken axial symmetry, such as smectic-C phase, require that, for each given l, all $2l + 1$ terms corresponding to the possible m values are included in the calculation. Very recently, Shah and Ganesan[7] evaluated the bridging/looping fractions in a model of semicrystalline multiblock copolymers, where the crystalline block was taken as a semiflexible chain. In their model system, the orientation interaction is described by a Maier−Saupe mean-field potential. The resulting SCFT equations were solved using the numerical method proposed by Sullivan et al.[6]

In the current work, a new numerical implementation of SCFT of wormlike chains is introduced, focusing on the self-assembly of semiflexible diblock copolymers. The new numerical method is developed in the spirit of the usual real-space method. The basic idea is that because the orientation of a segment of the wormlike chains is described by a unit vector, **u**, the phase space of the problem can be mapped to the surface of a unit sphere plus the usual 3D space. In our numerical implementation, the **u** variable on a unit sphere is discretized using an icosahedron triangular mesh, and a finite volume algorithm[55] is employed to evaluate the Laplacian on the unit sphere, $\nabla^2_{\mathbf{u}}$. Using this strategy, the diffusion equation of the chain propagator $q(\mathbf{r},\mathbf{u},t)$ can be numerically solved using the usual real-space techniques. The advantage of this approach is that it does not require prior knowledge about the symmetry of the ordered phase. The solution of smectic-C phases, in which the nematic direction and lamellae normal do not coincident, can easily be obtained. As an application of this method, phase transition and phase diagram of semiflexible diblock copolymers are studied for the case with 1D spatial order. To the best of our knowledge, SCFT

solutions corresponding to smectic-C phases of semiflexible diblock copolymers have not been obtained in previous studies.

II. Theoretical Model and Numerical Algorithm

The model system consists of n monodisperse rod−coil diblock copolymers in a volume, V. The average number density of copolymers is then given by $\rho = n/V$. Each copolymer chain is characterized by a total contour length, L, and a diameter, D. The copolymer chain is further specified by the polymerization index, N, and a fixed segment length, a, which are related to the contour length, $L = Na$. The volume fraction of the rod block is f. The rodlike chains are modeled using the wormlike (semiflexible) chain model. In this model, the configuration of a polymer chain is represented by a space curve, $\mathbf{r}(t)$, where $t \in [0,1]$, and a dimensionless unit vector, $\mathbf{u}(t) = (\mathrm{d}\mathbf{r}(t))/(L\ \mathrm{d}t)$, specifies the tangent vector of the chain at contour location, t. The rigidity of the semiflexible chain is quantified by the local curvature, which is proportional to $|\mathrm{d}\mathbf{u}(t)/\mathrm{d}t|$.

In principle, the different blocks will experience orientation interactions and repulsive interactions, which are usually specified by Flory−Huggins interaction parameters. For simplicity, we will ignore the isotropic repulsion in the current model. Therefore, there is no chemical difference between rod and coil blocks. Furthermore, the polymer chain is assumed to be thin enough, that is, $L,a \gg D$, so that the Onsager second-virial approximation can be used to describe the orientation interactions between chain segments. In the Onsager model, the angle-dependent excluded-volume interaction between two segments, of length $L\ \mathrm{d}t$ and $L\ \mathrm{d}t'$ and orientations $\mathbf{u}$ and $\mathbf{u}'$, respectively, is given by $v(\mathbf{u},\mathbf{u}')\ \mathrm{d}t\ \mathrm{d}t'$, where $v(\mathbf{u},\mathbf{u}') = 2DL^2|\mathbf{u}\times\mathbf{u}'|$. The Onsager excluded-volume interactions between any two segments including rod−rod, rod−coil, and coil−coil enforce local alignment of the chains. Furthermore, the rod and coil segments are distinguished by a rigidity parameter, $\xi(t)$, which is a function of the chain contour variable, t. It should be noticed that the Onsager excluded-volume interaction is employed here for its simplicity. Extension of the numerical technique to more complicated rod−coil models is straightforward.

The partition function of the model system in a canonical ensemble can now be written down as

$$Z = \frac{1}{n!}\prod_{i=1}^{n}\int D\{\mathbf{r}_i,\mathbf{u}_i\}P\{\mathbf{r}_i,\mathbf{u}_i[0,1]\} \exp\left(-\rho G\int \mathrm{d}\mathbf{r}\int \mathrm{d}\mathbf{u}\int \mathrm{d}\mathbf{u}'\hat{\phi}(\mathbf{r},\mathbf{u})\hat{\phi}(\mathbf{r},\mathbf{u}')|\mathbf{u}\times\mathbf{u}'|\right) \quad (1)$$

where $G = L^2D\rho$ is a parameter proportional to the average polymer number density, ρ. For the wormlike chain model, the probability density of the end of chain with contour length t, at position $\mathbf{r}$ and tangent vector $\mathbf{u}$ is given by

$$P\{\mathbf{r}_i,\mathbf{u}_i[0,1]\} \propto \prod_t \boldsymbol{\delta}\left[\mathbf{u}_i(t)^2 - 1\right] \times \exp\left[-\frac{1}{2N}\int_0^1 \mathrm{d}t\ \kappa(t)\left(\left|\frac{\mathrm{d}\mathbf{u}_i(t)}{\mathrm{d}t}\right|^2\right)\right] \quad (2)$$

where $(1/(2N))\ \int_0^1 \mathrm{d}t\ \kappa(t)(|\mathrm{d}\mathbf{u}_i(t)/\mathrm{d}t|^2)$ is the energy penalty for local chain bending. The product of delta function in eq 2 constraints the modus of $\mathbf{u}_i(t) = (1/Na)(\mathrm{d}/\mathrm{d}t)\mathbf{r}_i(t)$ to unity so that the total contour length is kept constant, L. The bending rigidity of the segments is controlled by $\kappa(t)$. The rigidity modulus, $\xi(t) = \kappa(t)/N$, is a measure of the rigidity of semiflexible chains. $\hat{\phi}(\mathbf{r},\mathbf{u}) = (1/\rho)\ \sum_{i=1}^{n}\int_0^1 \mathrm{d}t_i\ \delta(\mathbf{r} - \mathbf{r}_i(t_i))\delta(\mathbf{u} - \mathbf{u}_i(t_i))$ is the microscopic contour-averaged total segment density operator. Following a standard field theoretical approach, the free energy functional of the system is obtained

$$\frac{F}{V} \propto \frac{G}{V}\left[\frac{G}{(\int \mathrm{d}\mathbf{u})^2}\int \mathrm{d}\mathbf{r}\int \mathrm{d}\mathbf{u}\int \mathrm{d}\mathbf{u}'\phi(\mathbf{r},\mathbf{u})\phi(\mathbf{r},\mathbf{u}')|\mathbf{u}\times\mathbf{u}'| - \frac{1}{\int \mathrm{d}\mathbf{u}}\int \mathrm{d}\mathbf{r}\int \mathrm{d}\mathbf{u}W(\mathbf{r},\mathbf{u})\phi(\mathbf{r},\mathbf{u})\right] - G\ln\frac{Q}{V} + G\ln G \quad (3)$$

$\phi(\mathbf{r},\mathbf{u})$ is the dimensionless contour-averaged total segment density function, which equals the statistical average $\langle\hat{\phi}(\mathbf{r},\mathbf{u})\rangle$ of the microscopic density. The function $W(\mathbf{r},\mathbf{u})$ is the potential field generated by all polymers in the system. The SCFT equations are obtained by minimizing the free energy functional (eq 3) with respect to the field variables $\phi(\mathbf{r},\mathbf{u})$ and $W(\mathbf{r},\mathbf{u})$. Carrying out such a minimization leads to the following set of coupled SCFT equations

$$W(\mathbf{r},\mathbf{u}) = 2G\int \mathrm{d}\mathbf{u}'\phi(\mathbf{r},\mathbf{u}')|\mathbf{u}\times\mathbf{u}'| \quad (4)$$

$$\begin{aligned}\phi_{\mathrm{rod}}(\mathbf{r},\mathbf{u}) &= \tfrac{V}{Q}\textstyle\int_0^f \mathrm{d}t\ q(\mathbf{r},\mathbf{u},t)q^+(\mathbf{r},\mathbf{u},t)\\ \phi_{\mathrm{coil}}(\mathbf{r},\mathbf{u}) &= \tfrac{V}{Q}\textstyle\int_f^1 \mathrm{d}t\ q(\mathbf{r},\mathbf{u},t)q^+(\mathbf{r},\mathbf{u},t)\\ \phi(\mathbf{r},\mathbf{u}) &= \phi_{\mathrm{rod}}(\mathbf{r},\mathbf{u}) + \phi_{\mathrm{coil}}(\mathbf{r},\mathbf{u})\end{aligned} \quad (5)$$

where the function $q(\mathbf{r},\mathbf{u},t)$ is an end-segment distribution function, which specifies the probability of finding tth segment at a spatial position $\mathbf{r}$ with orientation $\mathbf{u}$. This function satisfies the following Fokker−Planck (diffusion) equations and a set of initial conditions[56,57]

$$\frac{\partial}{\partial t}q(\mathbf{r},\mathbf{u},t) = \left[-L\mathbf{u}\cdot\nabla_{\mathbf{r}} + \frac{1}{2\xi(t)}\nabla_{\mathbf{u}}^2 - W(\mathbf{r},\mathbf{u})\right]q(\mathbf{r},\mathbf{u},t) \quad q(\mathbf{r},\mathbf{u},0) = 1$$

$$\frac{\partial}{\partial t}q^+(\mathbf{r},\mathbf{u},t) = \left[-L\mathbf{u}\cdot\nabla_{\mathbf{r}} - \frac{1}{2\xi(t)}\nabla_{\mathbf{u}}^2 + W(\mathbf{r},\mathbf{u})\right]q^+(\mathbf{r},\mathbf{u},t) \quad q^+(\mathbf{r},\mathbf{u},1) = 1 \quad (6)$$

In the above expressions, Q is the single chain partition function, which is given by

$$Q = \frac{\int \mathrm{d}\mathbf{u}\int \mathrm{d}\mathbf{r}q(\mathbf{r},\mathbf{u},1)}{\int \mathrm{d}\mathbf{u}} \quad (7)$$

Equations 4−7 constitute a set of SCFT equations describing the statistical thermodynamics of semiflexible diblock copolymers. The self-consistent procedure to solve this set of SCFT equations, as given in ref 6, is similar to the numerical procedure of solving SCFT equations of Gaussian chains. The algorithm consists of randomly generating initial values of fields $W(\mathbf{r},\mathbf{u})$. With the fields given, the diffusion-like equations (eq 6) can be solved to obtain the propagators. Next, polymer densities are calculated according to eq 5, and new fields $W(\mathbf{r},\mathbf{u})$ are generated using eq 4 combined with simple mixing method for the successive iteration of fields. The iteration is carried out until the free energy and fields become self-consistent. In what follows, we solve the above SCFT equations (eqs 4−7) in 1D spatial space. Namely, the densities are assumed to vary along the z axis. However, the segment orientation is still 3D, represented by a vector $\mathbf{u}$ on the surface of a unit sphere. Compared with the SCFT equations of Gaussian chains, the diffusion equation, eq 6, is more

expensive and difficult to be numerically solved because the chain propagator $q(\mathbf{r},\mathbf{u},t)$ has two additional internal coordinates. In fact, the most expensive procedure in wormlike chain SCFT equations is the computation of the diffusion equation of $q(\mathbf{r},\mathbf{u},t)$. Numerical solutions of the diffusion equation (eq 6) have been limited. A numerical method is based on expanding the $\mathbf{u}$-dependent quantities in terms of spherical harmonic functions, $Y_{l,m}(\mathbf{u})$[6,7]

$$q(\mathbf{r},\mathbf{u},t) = \sum_{l,m} q_{l,m}(\mathbf{r},t)\, Y_{l,m}(\mathbf{u}) \tag{8}$$

Therefore, the orientation dependence is now described by the spherical harmonic coefficients. The Fokker−Planck equation for $q(\mathbf{r},\mathbf{u},t)$ is replaced by a set of coupled equations for $q_{l,m}(\mathbf{r},t)$. This set of equations is quite complicated. For the simplest case of 1D ordered phases, it is necessary to solve $q_{l,m}(\mathbf{r},t)$ with sufficient resolution in four coordinates spanned by l, m, z, and t. To proceed, further simplifications have been made in the computations. For example, Duchs and Sullivan[6] limited the liquid crystal phase to axially symmetric ones (disordered, nematic, and smectic-A). The azimuthal symmetry of these phases ensures that $m = 0$, and thus the solution of SCFT equations can be obtained. However, the possibility of semctic-C phase is excluded when $m = 0$ is assumed.

In what follows, we introduce an alterative real-space method for the solution of the diffusion equation for semiflexible chain propagation. The essence of the method is to discretize the orientation variable on the surface of a unit sphere using a set of nearly uniform triangular lattice points. This method has been used in our previous studies of the self-assembly of diblock copolymers on a sphere.[55] Specifically, the surface of a unit sphere is triangulated with $M = 362$ vertexes. The orientation variable is then presented by the coordinates of these lattice points, $\mathbf{u}[M] = (u_{mx},u_{my},u_{mz})$. The advantage of this real-space method is that the $\mathbf{u}$ dependence is resolved in the 3D space. The inclusion of phases without axial symmetry is straightforward. From a numerical algorithm point of view, at given values of $\mathbf{r}$ and t, $q(\mathbf{r},\mathbf{u},t)$ can be treated as a field of M vertexes on the sphere. The rotational diffusion operator of $q(\mathbf{r},\mathbf{u},t)$, that is, the Laplacian on the unit spherical surface, $\nabla^2_{\mathbf{u}}q(z,\mathbf{u},t)$, can be specified using a finite volume algorithm, as adopted in our previous work.[55] Therefore, eq 6 can be solved in real space by performing a forward time centered space scheme and the finite volume algorithm for $\nabla^2_{\mathbf{u}}q(z,\mathbf{u},t)$.

To obtain solutions of nematic, smectic-A, and smectic-C phases and construct the phase diagram, we began the calculation with an initial angle between the nematic director and the z axis, which ranges from 0 to $\pi/2$ by a step of $\pi/18$. Moreover, to avoid the influence of box size along the z direction, each minimization of the free energy is iterated with respect to a range of L_z: $(0.5\sim2)d/L$, where d is the period of the ordered phase and L_z is the simulation size of the system. For the given initial angle and box size, the system will adjust the orientation of rigid blocks to an equilibrium value of tilt angle defined as θ_0. In general, the equilibrium tilting angle θ_0 is not the same as the initial guess value. For the final stable phase structure, the equilibrium period and tilt angle are determined by minimization of the free energy with respect to L_z and θ_0. For the results presented below, calculations are performed on a 1D grid with periodic boundary conditions. The spatial discretization is specified by $dz = 0.02L$, for this given spatial discretization (dz), we test the solution accuracy for different contour length discretizations (dt). For example, when we change dt from 1/1500 to 1/900, the solution converges, and the phase structure does not change. Therefore, we set the contour discretization to be $dt = 1/900$ and ensure that the phase structure is trustable.

III. Results and Discussion

In the current study, the rod−coil diblock copolymers are specified by a rigidity function $\xi_{\mathrm{rod}}(t) = 10.0$ and $\xi_{\mathrm{coil}}(t) = 0.1$ for the rod and coil blocks, respectively. This set of parameters is chosen such that the model represents diblock copolymers with rigid and flexible blocks. Furthermore, these parameters are identical to the ones used by Duchs and Sullivan[6] so that a direct comparison with their results can be made. As a first application of our real-space implementation of the SCFT for semiflexible rod−coil diblock copolymers, we focus on the simple case where the densities vary in the z direction, that is, 1D (1D) space, although extensions to 2D and 3D are straightforward. In the parameter space considered, solutions of different liquid crystal structures, such as nematic, smectic-A and smectic-C, are found for different values of G and f. To investigate the orientational structure of the smectic phases, orientational order parameters are defined. Because the excluded-volume interaction favors local alignment of the chains so that $|\mathbf{u}\times\mathbf{u}'| = 0$, a preferred orientation, $\mathbf{n}$, termed the nematic director, is selected by the system. We note that the rods were treated as being aligned perfectly along $\mathbf{n}$ in the Semenov−Vasilenko model,[43] and thus orientation fluctuations are ignored. In general, not all rods are aligned to the same direction, but rather their orientation is described by a distribution function. The nematic director, $\mathbf{n}$, can be identified as the peak position in this distribution function. The distribution function of a rigid polymer is given by the position- and orientation-dependent concentration $\phi(z,\mathbf{u})$. We should note that in this article the probability distribution of molecular orientations with respect to the nematic director (θ) is relatively narrow with two peaks at $\theta = 0$ and π because of the Onsager model employed in the calculations. In this case, biaxial effects of the smectic-C phase are quite small quantitatively and thus can be ignored. Compared with the Gaussian chain system, where the order−disorder transition (ODT) is determined by position-dependent densities, there are two types of order parameters to describe the phase behavior of semiflexible diblock copolymers: one is z-dependent density $\phi(z)$, and the other corresponds to the two $\mathbf{n}$-dependent order parameters $\overline{P}_1(z)$ and $\overline{P}_2(z)$, defined by

$$\overline{P}_{1,\beta}(z) = \frac{\int \mathrm{d}\mathbf{u}\, \phi_\beta(z,\mathbf{u}) \cos\theta}{\int \mathrm{d}\mathbf{u}\, \phi_\beta(z,\mathbf{u})}$$

$$\overline{P}_{2,\beta}(z) = \frac{\int \mathrm{d}\mathbf{u}\, \phi_\beta(z,\mathbf{u}) \left[\frac{1}{2}(3\cos^2\theta - 1)\right]}{\int \mathrm{d}\mathbf{u}\, \phi_\beta(z,\mathbf{u})} \tag{9}$$

where β indicates the segment species and θ is the angle between a segment axis and the nematic direction, $\mathbf{n}$. $\overline{P}_{1,\beta}(z)$ describes the average spatial direction in which segments β are oriented, and $\overline{P}_{2,\beta}(z)$ characterizes the overall degree of orientational order. Using this set of order parameters, $\phi(z)$ and $\overline{P}_2(z)$, the liquid crystalline phases of rod−coil block copolymers can be distinguished. For instance, the isotropic and nematic phases have uniform spatial distribution of density, but the nematic phase has an ordered orientation as a result of the rod alignment. In the smectic phases, both the orientational and positional orderings are observed. Dependent on the angle between the nematic director, $\mathbf{n}$, and the lamellae normal, θ_0, the smectic-A ($\theta_0 = 0$) and smectic-C ($\theta_0 \neq 0$) can be identified.

A. Comparison with the Spherical Harmonic Method. As a first example of application, 1D liquid crystalline phases of rod−coil diblock copolymers are studied using the real-space method. This study also serves as a test of the accuracy of our numerical method. Specifically, a rod−coil diblock copolymer

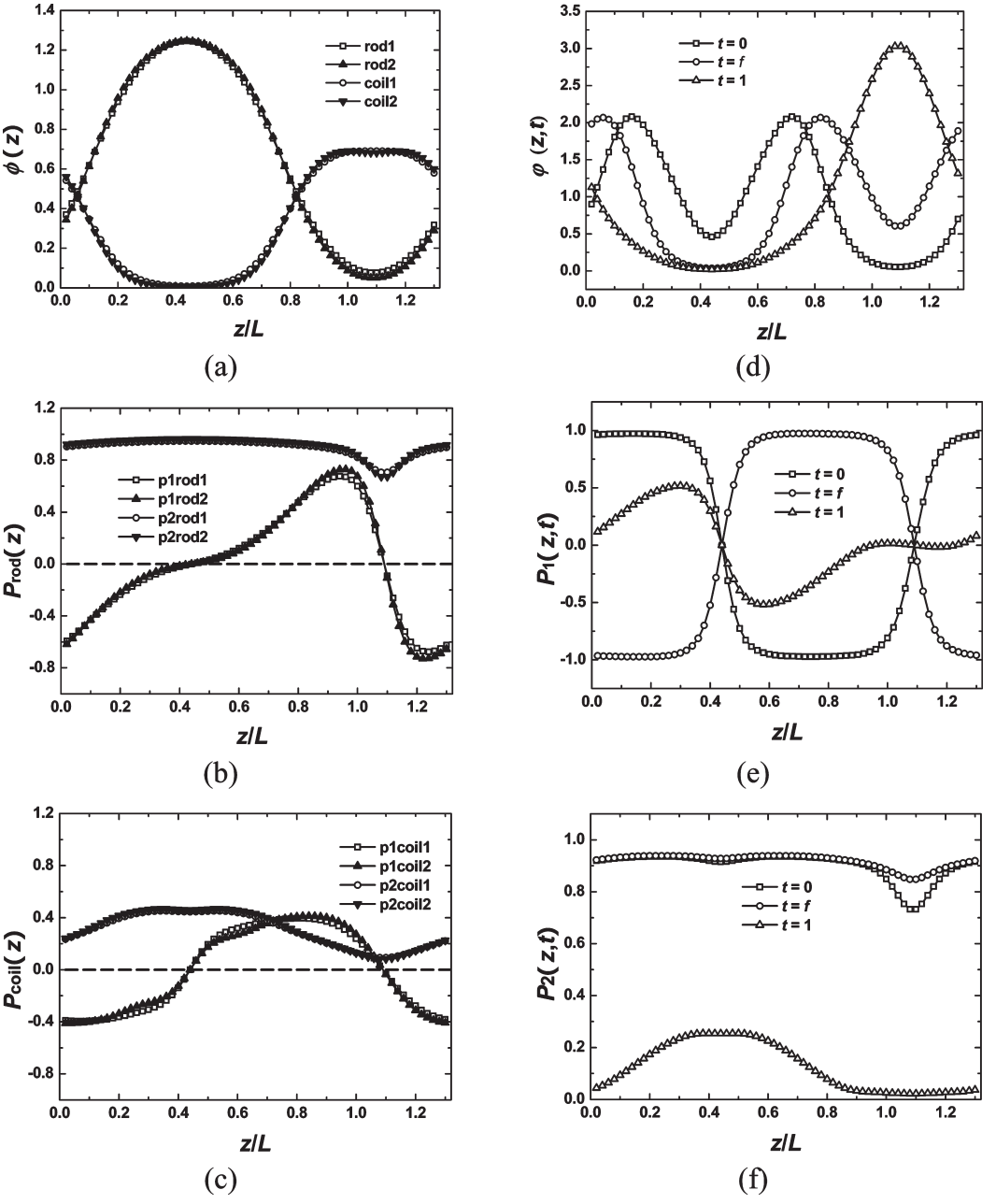

Figure 1. Segment density and order parameter distributions of a smectic-A phase with $f = 2/3$, $\xi_{rod}(t) = 10.0$, $\xi_{coil}(t) = 0.1$, $G = 20$, and period $1.30L$. In a−c, the last number, 1 or 2, in the code indicates results from the real-space and spectral methods, respectively. (a) Density distribution of rods and coils $\phi_{rod}(z)$ and $\phi_{coil}(z)$. (b) Orientational distribution of rods $\overline{P}_{1,rod}(z)$ and $\overline{P}_{2,rod}(z)$. (c) Orientational distribution of coils $\overline{P}_{1,coil}(z)$ and $\overline{P}_{2,coil}(z)$. Density and orientation distribution of special segments are shown in d−f by real-space method. (d) Density distribution of $\varphi(z,t = 0)$, $\varphi(z,t = f)$, and $\varphi(z,t = 1)$. (e) Orientational distribution of $\overline{P}_{1,t=0}(z)$, $\overline{P}_{1,t=f}(z)$, and $\overline{P}_{1,t=1}(z)$. (f) Orientational distribution of $\overline{P}_{2,t=0}(z)$, $\overline{P}_{2,t=f}(z)$, and $\overline{P}_{2,t=1}(z)$.

system with $f = 2/3$ and $G = 20$ is examined. This system is chosen because it has been studied using the spectral method by Duchs and Sullivan.[6] Therefore, a direct comparison of the results from the two numerical implementations can be made. In Figure 1a, the density distributions of rigid and flexible blocks for a smectic-A phase are plotted, showing excellent agreement between the two numerical methods. From these density distributions, we can conclude that the coil segments are almost expelled from the rod-rich domain, whereas a small amount of the rod segments is present in the coil-rich domain. Therefore, the rigidity of the blocks has a strong effect on the degree of segregation. The orientation order of the block copolymers is contained in the distribution of the two order parameters defined in eq 9, which are shown in Figure 1b,c. From these orientation order parameter profiles, we can conclude that the rodlike blocks in the rod domain are strongly oriented parallel or antiparallel to the nematic direction, **n** (the z axis), in the smectic-A phase (Figure 1b). However, a weaker orientation order is observed in the coil domain (Figure 1c). Both $\overline{P}_{2,rod}$ and $\overline{P}_{2,coil}$ exhibit maxima (minima) in the regions of high (low) rod density. $\overline{P}_{1,rod}$ and $\overline{P}_{1,coil}$ vanish in the middle of the rod-rich and coil-rich domains, which is a result of the axis symmetry of the rodlike polymers. It should be noticed that there are noticeable differences between our Figure 1 and the plots shown in the paper of Duchs and Sullivan,[6] although the same parameters for the diblock copolymers are used. Specifically, the plots shown by Duchs and Sullivan are more gradual than Figure 1. The origin of this difference can be traced to the number of basis functions used in the calculation of the

interaction potential. Indeed, we have compared values of the interaction potential, $v(\mathbf{u},\mathbf{u}') = 2DL^2|\mathbf{u} \times \mathbf{u}'|$, using our real-space method and the spherical harmonics expansion and found that truncation of the expansion to $l = 2$ does not give an accurate representation of the interaction potential. The need for a larger number of basis functions has been noticed by Duchs and Sullivan, as well as by Chen.[58] In our calculations, a larger number of spherical-harmonic terms, such as up to $l = 12$, have been used so that the results from the two numerical methods are consistent (Figure 1).

To investigate the detailed structure of the smectic-A phase, the distribution function at position z for the segment at t along the chain $\varphi(z,t)$ is calculated according to the SCFT

$$\varphi(z,t) = \frac{V \int d\mathbf{u}\, q(z,\mathbf{u},t)q^+(z,\mathbf{u},t)}{Q \int d\mathbf{u}} \tag{10}$$

The corresponding orientational order parameter distributions for the segment at t along the chain are given by

$$\overline{P}_{1,t}(z) = \frac{\int d\mathbf{u}\, q(z,\mathbf{u},t)q^+(z,\mathbf{u},t)\ cos\ \theta}{\int d\mathbf{u}\, q(z,\mathbf{u},t)q^+(z,\mathbf{u},t)}$$

$$\overline{P}_{2,t}(z) = \frac{\int d\mathbf{u}\, q(z,\mathbf{u},t)q^+(z,\mathbf{u},t)\left[\frac{1}{2}(3\ cos^2\ \theta - 1)\right]}{\int d\mathbf{u}\, q(z,\mathbf{u},t)q^+(z,\mathbf{u},t)} \tag{11}$$

These distribution functions at the two ends ($t = 0$ and 1) and the junction ($t = f$) of the diblock copolymers are plotted in Figure 1d−f. It is apparent that the smectic-A phase possesses a partial bilayer structure, consistent with the conclusion from a previous theoretical study[54] and experiment.[1] The nature of the bilayer structure can be obtained from the segment distributions. The segment density of the rod ends, $\varphi(z,t = 0)$, exhibits two maxima separated by a distance of $0.56L$ (Figure 1d), which is slightly less than the length of the rigid blocks, $2/3L$. At the same time, the orientation order parameter at the rod ends, $\overline{P}_{1,t=0}(z)$, reaches its maximum values, $\overline{P}_{1,t=0} = \pm 1$, at peak positions of $\varphi(z,t = 0)$ (Figure 1e). The segment density distribution of the junctions ($t = f$) exhibits two peaks that are separated by a distance of $0.76L$, slightly larger than the rod length (Figure 1d). The orientation order parameter at the junctions, $\overline{P}_{1,t=f}(z)$, again reaches its maximum values, $\overline{P}_{1,t=f} = \pm 1$, at peak positions of the segment distribution (Figure 1e). The domain spacing of the rigid domain is found to be approximately $0.66L$, which is in agreement with the rod length of $2/3L$. From these observations, it can be concluded that the rod blocks are in almost complete oriented state in the rod domain. However, the segment density distribution at the coil terminals $\varphi(z,t = 1)$ exhibits one peak in the middle of the coil domain (Figure 1d), which is consistent with an earlier study.[54] The single-peak behavior is quite different from the double-peak behavior of the rod-end ($t = 0$) and rod−coil junction ($t = f$) distributions. The overall degree of orientational order is characterized by $\overline{P}_{2,t}(z)$, which is shown for the different segments in Figure 1f. Different orientation behaviors are observed in the rod and coil domains. As expected, maximum orientation order occurs in the rod domain, as shown by the distribution function at $t = 0$ and $t = f$. Meanwhile, the coil ends possess minimum orientation order, especially in the coil domain. It is interesting to observe that there is a substantially induced orientation order of the coil segments, as shown by the distribution $\overline{P}_{2,t=1}(z)$ in the rod domain in Figure 1f.

B. Smectic-C. One distinct advantage of our real-space method is that it is straightforward to treat general liquid crystalline phases such as smectic-C, in which the rod orientation is not parallel to the lamellae normal. As an example of structures with broken axial symmetry, the smectic-C phase for rod−coil diblock copolymers with $f = 0.65$ is examined in this section. It should be noticed that SCFT solutions for smectic-C phases have not been obtained in previous studies.[6] To obtain a solution of smectic-C phase, an initial nonzero tilt angle between the nematic director, **n**, and the z-axis is needed. In the numerical calculation, this initial angle ranges between 0 and 90° with an interval of 10°. For a given initial angle, solutions of the SCFT equations are obtained. For a given smectic-C solution, the nematic director, **n**, and the tilt angle are easily determined from the distribution of rod segments, $\phi_{rod}(z,\mathbf{u})$. The numerical results show that the smectic-C phase occurs when G exceeds 16. In the case of $G = 16$, the tilt angle for smectic-C phase is $\theta_0 = 30°$ with an equilibrium period of $d = 1.14L$.

The structure of the smectic-C phase can be examined using the distribution functions of the segment density and orientation order parameters, which are shown in Figure 2. The first feature to notice is that the density and orientation distributions of rods and coils (Figure 2a−c) are similar to those of the smectic-A phase (Figure 1a−c). In the middle of the rod domain, the coils are almost completely expelled, and both the rod and coil blocks possess strong orientation order along the nematic director, **n** (Figure 2c). In particular, the rods are aligned with the nematic director, whereas the coils acquire certain degree of orientation order in the rod domain. In the middle planes of the rod and coil domains, the average first-order orientation order parameter, $\overline{P}_1(z)$, vanishes, indicating that the rod orientation is symmetric about the nematic director (Figure 2b). The segment density distributions of the rod ends ($t = 0$), junctions ($t = f$), and coil ends ($t = 1$) are shown in Figure 2d−f. The rod ends and junctions exhibit two peaks close to the rod−coil interface. The distance along the z axis between the two peaks in the junction distribution is $0.76L$, whereas the spacing between the two peaks in the rod-end distribution is $0.44L$. The orientation of the segments at the rod end ($t = 0$) and the junction ($t = f$) reverses its direction in the middle of the rod domain, as shown in Figure 2e. The antiparallel arrangement of the rod-ends and junctions suggests a large degree of interdigitation of the rod blocks. The coil-end distribution ($t = 1$) exhibits one peak (Figure 2d) in the middle of the coil domain with a weak degree of orientation order (Figure 2f). These distribution functions show that the smectic-C phase is also a partial bilayer structure, similar to that of the smectic-A phase shown in Figure 1.

The thickness of the rod domain is about $0.6L$ along the z axis, as estimated from the distribution function (Figure 2d). Because the rod length is $0.65L$ and the tilt angle is 30°, the predicted rod-domain thickness is $0.65L \times \cos 30° = 0.56L$ which is smaller than the observed domain thickness of $0.6L$. This observation implies that the rigid rods are not in a perfect alignment along the nematic director. There is some degree of tilt angle distribution in the system. This behavior is different from that observed in the smectic-A phase (Figure 1), in which the rod-domain thickness agrees with the rod length, implying a more complete alignment of the rods. The occurrence of the smectic-C at large values of G can be attributed to the fact that stronger the excluded-volume effect favors more closely packed rods. However, stronger rod packing leads to a smaller interfacial area per copolymer chain, thus increasing the stretching energy of the coils. To reduce this stretching energy of coils, the rigid segments tilt

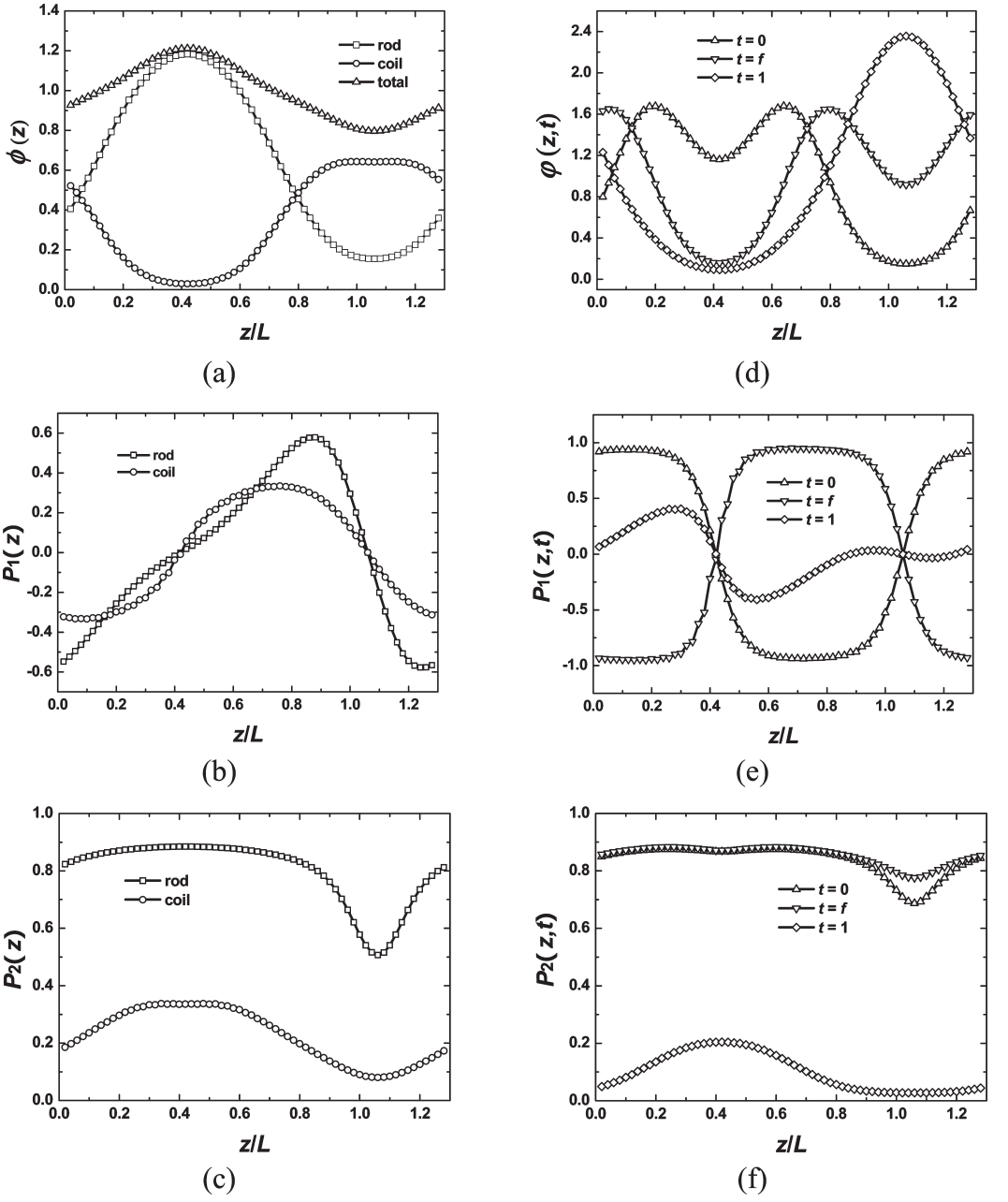

Figure 2. Segment density and order parameter distributions of a smectic-C phase with $f = 0.65$, $\xi_{rod}(t) = 10.0$, $\xi_{coil}(t) = 0.1$, $G = 16$, $\theta_0 = 30$, and period $1.28L$. (a) Density distribution of rods and coils $\phi_{rod}(z)$ and $\phi_{coil}(z)$. (b) Orientational distribution of $\overline{P}_{1,rod}(z)$ and $\overline{P}_{1,coil}(z)$. (c) Orientational distribution of $\overline{P}_{2,rod}(z)$ and $\overline{P}_{2,coil}(z)$. (d) Density distribution of $\varphi(z,t = 0)$, $\varphi(z,t = f)$ and $\varphi(z,t = 1)$. (e) Orientational distribution of $\overline{P}_{1,t=0}(z)$, $\overline{P}_{1,t=f}(z)$, and $\overline{P}_{1,t=1}(z)$. (f) Orientational distribution of $\overline{P}_{2,t=0}(z)$, $\overline{P}_{2,t=f}(z)$, and $\overline{P}_{2,t=1}(z)$.

by an angle to the lamellae normal, forming smectic-C phase. Therefore the existence of the smectic-C in our model is a result of the competitive effects between the excluded-volume interactions for rigid segments and stretching energy of coil blocks. The assumption of strict alignment of rods, as employed previously by Matsen and Barrett,[43] only applies to the smectic-A phase.

For rod−coil diblock copolymers with $f = 0.65$, the smectic-C phase is stable for $G \geq 16$. The equilibrium tilt angle, θ_0, and period, d, depend on the excluded-volume interaction. Large values of G lead to an increase in tilt angle and a decrease in the lamellae period, d. Specifically, for $G = 16$, 18, and 20, the tilt angle is found to be $\theta_0 = 30$, 50, and 70°, whereas the equilibrium lamellae period is $d = 1.14L$, $1.06L$, and $0.56L$. This observation can be attributed to the competition between the excluded-volume interaction of the rods and the stretching energy of the coils. The increase in G drives the rigid blocks to align more closely at the cost of the coils stretching entropy. A large tilt angle can alleviate this frustration by increasing the interfacial area per chain while keeping the same degree of packing. The density and orientation distribution of rods and coils (figures not shown here) are similar to those of $G = 16$ (Figure 2). For example, in the center of the rod domain, the coils are expelled, and both rods and coils have high orientational order. The smectic-C also exhibits a partial bilayer structure, where the rod blocks have almost complete interdigitation but coil blocks mainly form a bilayer configuration. The density distribution of the rigid and flexible blocks exhibits no sharp interfaces, indicating that the interfacial energy is smaller than that of the monolayer. The partial bilayer structure gives the coils more space in favor of their stretching energy.[33]

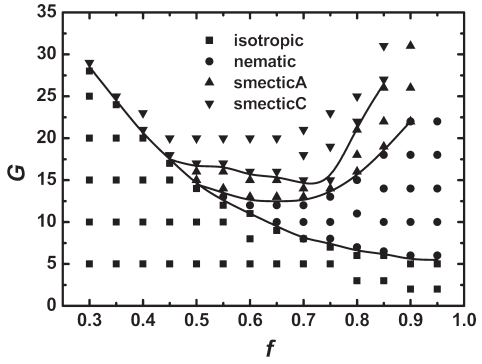

Figure 3. Phase diagram of rod−coil diblock copolymers. The solid lines are guide to the eye.

C. Phase Diagram. The SCFT solutions for the different phases (disordered, nematic, smectic-A, and smectic-C) allow us to construct a phase diagram for the model rod−coil diblock copolymers. In what follows, the phase diagram in the plane of orientational interactions versus copolymer compositions ($G - f$) for the rod−coil diblock copolymers with $\xi_{rod}(t) = 10.0$ and $\xi_{coil}(t) = 0.1$ is presented (Figure 3). For the purpose of a direct comparison, the model parameters are the same as the those employed by Duchs and Sullivan,[6] who have considered three phases (disordered, nematic, and smectic-A) in their calculations using a spectral method.

Isotropic−Nematic Transition ($I-N$). In the coil−coil diblock copolymers, the disordered phase is spatially homogeneous without orientational order. In the case of rod−coil diblock copolymers, orientational order may persist in a spatially homogeneous phase because of the strong anisotropic interactions between the rod blocks, leading to the formation of the nematic phase. In our model, the isotropic-to-nematic (I−N) transition can be discerned from the density and orientation order parameters. Specifically, an isotropic phase corresponds to the trivial solution $\phi(z) =$ const and $\overline{P}_2(z) = 0$, whereas a nematic phase is characterized by $\phi(z) =$ const and $\overline{P}_2(z) \neq 0$. In the phase diagram (Figure 3), the nematic phase occupies a wide region at high rod volume fractions, and it narrows upon increasing coil volume fractions until the nematic disappears at a triple point. After that, a direct transition from isotropic to smectic-A phase occurs. The I−N transition is in excellent agreement with the result obtained by spectral method;[6] however, the triple point in Figure 3 appears at smaller values of G and high rod fraction, f. It is due to the slightly different treatments of orientational interaction potential, as discussed in above subsection A. In addition, this result is in qualitative agreement with the predictions of Reenders and ten Brinke[36] using a Landau theory as well as an experimental phase diagram of a model rod−coil diblock copolymer in weak segregation limit from Olsen and Segalman.[25] In contrast, Pryamitsyn and Ganesan[44] observed only a narrow nematic region in their SCFT simulations. It is noticed that in their model, the orientation interaction parameter, μ, is incorporated as a renormalization of the χ parameter. In their simulations, a fixed ratio of $\mu/\chi = 4$ was used. It is likely that this ratio is much smaller than the experimental measurement of μ and χ by Olsen et al.,[27] where μ was found to be roughly 50 times larger than χ in the experimental temperature range. In another related study, Matsen and Barrett[43] employed the Semenov−Vasilenko model and constrained the rod orientation to a preferred direction. Therefore, the isotropic phase was ruled out from their 1D phase diagram in the spatial homogeneous phase space, and this treatment broke down at high coil volume fractions. In a recent study, Jiang and Wu[59] have focused on the I−N transition in athermal solutions of rod−coil diblock copolymers by a hybrid method, incorporating the scaled-particle theory for semiflexible chains with two-chain Monte Carlo simulations. They predicted that the driving force of the I−N transition was the competition between orientational and packing entropies, which is a conclusion from the current study.

Nematic-to-Smectic-A Transition ($N-A$). In the phase diagram shown in Figure 3, a nematic-to-smectic-A transition is observed when the volume fraction of rod lies in the range $0.5 \leq f \leq 0.9$. The value of G for the N−A transition is slightly lower than that observed in ref 6, which is reasonable because of the slightly different treatments of orientational interaction potential, as discussed in subsection A. The N−A phase boundary shows a minimum value of G at $f = 0.7$, and G increases very slowly when $f < 0.7$. However, the N−A boundary raises sharply when $f > 0.7$. Qualitatively similar phase behavior of the N−A transition was predicted by Pryamitsyn and Ganesan[44] and by Matsen and Barrett.[43] On the contrary, there was only N−C transition in the 2D Landau free energy expansion calculations by Reenders and ten Brinke,[36] where the smectic-A phases were absent because of the breakdown of free energy expansion in the order parameters. Therefore, it can be concluded that when the liquid crystal interaction is strong enough to drive the system to form nematic phases, further increasing the orientational or Flory−Huggins interactions will lead to the formation of a smectic-A phase because of the dominant role of the interfacial energy. We should note that the end effects described in refs 53−54 are omitted in this article to compare with ref 6. Therefore, in the limit of $f \rightarrow 1$, that is, homogeneous rigid polymers, smectic phases do not occur in the current model.

Smectic-A-to-Smectic-C Transition ($A-C$). When the volume fraction of the coils is high or the orientation interaction is stronger, the smectic-C phase occurs because of the stretching energy of the coils. As shown in the phase diagram (Figure 3), the smectic-C phase occupies a large region at large values of G when the coil volume fraction is relatively high. This behavior is consistent with previous theoretical studies. As G is increased, a smectic-A-to-smectic-C (A−C) transition exists above a nematic-to-smectic-A transition line in the region of $0.45 \leq f \leq 0.85$. Using a scaling argument, Halperin[33] predicted a first-order A−C transition due to the competition between the deformation free energy of flexible blocks and the interfacial free energy of rigid blocks. The first-order nature of the A−C transition is contained in the equilibrium tilt angle, which jumps from zero in the smectic-A phase to a large nonzero angle ($\theta_0 \geq 30°$) in the smectic-C phase. This observation is in qualitative agreement with the prediction of Halperin. The A−C transition boundary shown in Figure 3 can be divided into two parts: one ranges from $f = 0.45$ to 0.75 where the A−C transition boundary is sensitive to the orientational interaction, G; the other part ranges from $f = 0.75$ to 0.85 where the A−C transition boundary is sensitive to the coil volume fraction. Similar to the 1D phase diagram calculated by Masten and Barrett,[43] a large area of smectic-C phase was found when ν (coil-to-rod length ratio, defined as $\sqrt{6Rg_{coil}}/L_{rod}$) was relatively small. However, Pryamitsyn and Ganesan[44] predicted that the rod−coil diblock copolymers with intermediate values of f and $\nu = 0.15$ have an A−C transition boundary that is only sensitive to the coil volume fraction. Experimental study on the phase behavior of rod−coil diblock copolymers in the weak segregation limit revealed that a smectic-A phase could

transform to a smectic-C phase as the temperature decreased, that is, orientational interactions between rigid blocks are increased.[25] This A−C transition was observed in model rod−coil copolymers with relatively high coil volume fraction, qualitatively in agreement with our theoretical results.

Isotropic-to-Smectic-C Transition (*I*−*C*). The phase diagram shown in Figure 3 also exhibits a direct transition from the isotropic phase to a smectic-C phase when the rod volume fraction is relatively small ($0.3 \leq f \leq 0.45$) and the value of G is high enough. The value of G for the I−C transition increases sharply as the coil volume fraction becomes larger, similar to the observation of the I−C transition by Pryamitsyn and Ganesan[44] in their 1D phase diagram. Experimental studies[18] have also revealed direct transitions from an isotropic phase to a smectic-C phase in a model rod−coil diblock copolymer system with high coil volume fractions. The I−C transition occurs when the nematic ordering interaction is stronger than the microphase separation interaction. Therefore, both theoretical and experimental results indicate that high coil volume fractions stabilize isotropic phase when the liquid crystal interaction is relatively weak. With the increase in orientational interactions, the isotropic phase can directly transform to a smectic-C phase, driven by the release of the stretching energy of the coils.

IV. Conclusions

A new real-space numerical method for SCFT of semiflexible polymers has been developed. The method is based on the observation that the orientation degree of freedom of the wormlike chain segment can be described by an angular variable, **u**, which is a 2D vector on the surface of a unit sphere. In the spirit of real-space numerical methods, the unit sphere is discretized using an icosahedron mesh. Furthermore, the Laplacian operator on the unit sphere is treated using a finite volume algorithm. This real-space numerical method allows the solution of the chain propagator, $q(\mathbf{r},\mathbf{u},t)$, of the semiflexible polymers. In particular, the orientation, **u**, of the rigid blocks is considered in 3D space, and thus the smectic-C phase and smectic-A phase can be treated at equal footing.

As a first example of application of the real-space numerical implementation of SCFT for wormlike chains, the phase behavior of a model rod−coil diblock copolymer is studied. To make direct comparison with previous studies, a simple model with Onsager excluded-volume interaction is employed in the current study. Numerical SCFT solutions corresponding to the typical liquid crystalline phases including nematic and smectic phases are obtained. Excellent agreement between the real-space and spectral methods has been achieved for the case of isotropic-to-nematic transitions.[6] One of the advantages of the real-space method is that the smectic-C phase can be conveniently treated, whereas the smectic-C phase presents a major problem in the spectral method.[6] The solutions of the different liquid crystalline phases allow us to construct a phase diagram of rod−coil diblock copolymers (Figure 3). The phase diagram in the G−f plane is in qualitative agreement with previously theoretical predictions.[36,43,44]

To our knowledge, the current work is the first attempt to solve the orientation **u**-dependent and position **r**-dependent SCFT equation of wormlike chains using a real-space numerical method. In particular, the Laplacian on the unit spherical surface, $\nabla^2_{\mathbf{u}}$, in chain propagator, $q(\mathbf{r},\mathbf{u},t)$, can be efficiently solved directly in real space with our previous proposed finite volume method. This numerical algorithm provides a simple and intuitive method to deal with SCFT equations of wormlike chains. Although the application of the method in this article is for liquid crystalline phases with 1D spatial order, this real-space method can be straightforwardly extended to high-dimensional variation of compositions for investigating complex liquid crystalline phase structures besides layered structures as well as to incorporation of other orientational interactions such as the Maier−Saupe interaction for thermotropic liquid crystal.

Acknowledgment. We acknowledge financial support from the National Basic Research Program of China (grant no. 2005CB623800) and funding from the NSF of China (grant nos. 20674012 and 20874020) is also acknowledged. A.-C.S. acknowledges the support from the Natural Science and Engineering Research Council (NSERC) of Canada.

References and Notes

(1) (a) Fredrickson, G. H.; Ganesan, V.; Drolet, F. *Macromolecules* **2002**, *35*, 16. (b) Fredrickson, G. H. *The Equilibrium Theory of Inhomogeneous Polymers*, 1st ed.; Oxford University Press: Oxford, U.K., 2006. (c) Shi, A. C. In *Developments in Block Copolymer Science and Technology*; Hamley, I., Ed.; Wiley: New York, 2004; p 265.
(2) (a) Matsen, M. W.; Schick, M. *Phys. Rev. Lett.* **1994**, *72*, 2660. (b) Guo, Z. J.; Zhang, G. J.; Qiu, F.; Zhang, H. D.; Yang, Y. L.; Shi, A. C. *Phys. Rev. Lett.* **2008**, *101*, 028301.
(3) Drolet, F.; Fredrickson, G. H. *Phys. Rev. Lett.* **1999**, *83*, 4317.
(4) Tzeremes, G.; Rasmussen, K. O.; Lookman, T.; Saxena, A. *Phys. Rev. E* **2002**, *65*, 041806.
(5) Matsen, M. W. *J. Chem. Phys.* **1996**, *104*, 7758.
(6) Duchs, D.; Sullivan, D. E. *J. Phys.: Condens. Matter* **2002**, *14*, 12189.
(7) Shah, M.; Ganesan, V. *J. Chem. Phys.* **2009**, *130*, 054904.
(8) Ganesan, V.; Khounlavong, L.; Pryamitsyn, V. *Phys. Rev. E* **2008**, *78*, 051804.
(9) Olsen, B. D.; Segalman, R. A. *Mater. Sci. Eng., R* **2008**, *62*, 37.
(10) Chen, J. T.; Thomas, E. L.; Ober, C. K.; Mao, G. P. *Science* **1996**, *273*, 343.
(11) Lee, M.; Cho, B. K.; Kim, H.; Yoon, J. Y.; Zin, W. C. *J. Am. Chem. Soc.* **1998**, *120*, 9168.
(12) Ryu, J. H.; Oh, N. K.; Zin, W. C.; Lee, M. *J. Am. Chem. Soc.* **2004**, *126*, 3551.
(13) Tenneti, K. K.; Chen, X. F.; Li, C. Y.; Tu, Y. F.; Wan, X. H.; Zhou, Q. F.; Sics, I.; Hsiao, B. S. *J. Am. Chem. Soc.* **2005**, *127*, 15481.
(14) Li, C. Y.; Tenneti, K. K.; Zhang, D.; Zhang, H. L.; Wan, X. H.; Chen, E. Q.; Zhou, Q. F.; Carlos, A. O.; Igos, S.; Hsiao, B. S. *Macromolecules* **2004**, *37*, 2854.
(15) Radzilowski, L. H.; Carragher, B. O.; Stupp, S. I. *Macromolecules* **1997**, *30*, 2110.
(16) Radzilowski, L. H.; Stupp, S. I. *Macromolecules* **1994**, *27*, 7747.
(17) Cho, B. K.; Chung, Y. W.; Lee, M. *Macromolecules* **2005**, *38*, 10261.
(18) Sary, N.; Brochon, C.; Hadziioannou, G.; Mezzenga, R. *Eur. Phys. J. E* **2007**, *24*, 379.
(19) Sary, N.; Rubatat, L.; Brochon, C.; Hadziioannou, G.; Ruokolainen, J.; Mezzenga, R. *Macromolecules* **2007**, *40*, 6990.
(20) Dai, C. A.; Yen, W. C.; Lee, Y. H.; Ho, C. C.; Su, W. F. *J. Am. Chem. Soc.* **2007**, *129*, 11036.
(21) Jenekhe, S. A.; Chen, X. L. *Science* **1998**, *279*, 1903.
(22) Mao, G. P.; Wang, J. G.; Clingman, S. R.; Ober, C. K.; Chen, J. T.; Thomas, E. L. *Macromolecules* **1997**, *30*, 2556.
(23) Lee, M.; Cho, B. K.; Kim, H.; Zin, W. C. *Angew. Chem., Int. Ed.* **1998**, *37*, 638.
(24) Lee, M.; Cho, B. K.; Kang, Y. S.; Zin, W. C. *Macromolecules* **1999**, *32*, 7688.
(25) Olsen, B. D.; Segalman, R. A. *Macromolecules* **2005**, *38*, 10127.
(26) Olsen, B. D.; Segalman, R. A. *Macromolecules* **2006**, *39*, 7078.
(27) Olsen, B. D.; Shah, M.; Ganesan, V.; Segalman, R. A. *Macromolecules* **2008**, *41*, 6809.
(28) Olsen, B. D.; Li, X. F.; Wang, J.; Segalman, R. A. *Macromolecules* **2007**, *40*, 3287.
(29) Segalman, R. A. *Mater. Sci. Eng., R* **2005**, *48*, 191.
(30) Lee, M.; Cho, B. K.; Zin, W. C. *Chem. Rev.* **2001**, *101*, 3869.
(31) Semenov, A. N.; Vasilenko, S. V. *Zh. Eksp. Teor. Fiz.* **1986**, *90*, 124.
(32) Semenov, A. N. *Mol. Cryst. Liq. Cryst.* **1991**, *209*, 191.
(33) Halperin, A. *Europhys. Lett.* **1989**, *10*, 549.

(34) Williams, D. R. M.; Fredrickson, G. H. *Macromolecules* **1992**, *25*, 3561.
(35) Holyst, R.; Schick, M. *J. Chem. Phys.* **1992**, *96*, 730.
(36) Reenders, M.; ten Brinke, G. *Macromolecules* **2002**, *35*, 3266.
(37) Bohbot-Raviv, Y.; Wang, Z. G. *Phys. Rev. Lett.* **2000**, *85*, 3428.
(38) Tang, P.; Qiu, F.; Zhang, H. D.; Yang, Y. L. *Phys. Rev. E* **2004**, *69*, 031803.
(39) Li, X. A.; Tang, P.; Qiu, F.; Zhang, H. D.; Yang, Y. L. *J. Phys. Chem. B* **2006**, *110*, 2024.
(40) Han, W. C.; Tang, P.; Li, X.; Qiu, F.; Zhang, H. D.; Yang, Y. L. *J. Phys. Chem. B* **2008**, *112*, 13738.
(41) Sides, S. W.; Kim, B. J.; Kramer, E. J.; Fredrickson, G. H. *Phys. Rev. Lett.* **2006**, *96*, 250601.
(42) Muller, M.; Schick, M. *Macromolecules* **1996**, *29*, 8900.
(43) Matsen, M. W.; Barrett, C. *J. Chem. Phys.* **1998**, *109*, 4108.
(44) Pryamitsyn, V.; Ganesan, V. *J. Chem. Phys.* **2004**, *120*, 5824.
(45) Chen, J. Z.; Zhang, C. X.; Sun, Z. Y.; Zheng, Y. S.; An, L. J. *J. Chem. Phys.* **2006**, *124*, 104907.
(46) Li, W.; Gersappe, D. *Macromolecules* **2001**, *34*, 6783.
(47) Hamm, M.; Goldbeck-Wood, G.; Zvelindovsky, A. V.; Fraaije, J. *J. Chem. Phys.* **2003**, *118*, 9401.
(48) Hamm, M.; Goldbeck-Wood, G.; Zvelindovsky, A. V.; Fraaije, J. *J. Chem. Phys.* **2004**, *121*, 4430.
(49) Horsch, M. A.; Zhang, Z. L.; Glotzer, S. C. *Phys. Rev. Lett.* **2005**, *95*, 056105.
(50) Diplock, R.; Sullivan, D. E.; Jaffer, K. M.; Opps, S. B. *Phys. Rev. E* **2004**, *69*, 062701.
(51) Movahed, H. B.; Hidalgo, R. C.; Sullivan, D. E. *Phys. Rev. E* **2006**, *73*, 032701.
(52) Netz, P. R.; Schick, M. *Phys. Rev. Lett.* **1996**, *77*, 302.
(53) Hidalgo, R. C.; Sullivan, D. E.; Chen, J. Z. Y. *Phys. Rev. E* **2005**, *71*, 041804.
(54) Hidalgo, R. C.; Sullivan, D. E.; Chen, J. Z. Y. *J. Phys.: Condens. Matter* **2007**, *19*, 376107.
(55) Tang, P.; Qiu, F.; Zhang, H. D.; Yang, Y. L. *Phys. Rev. E* **2005**, *72*, 016710.
(56) Morse, D. C.; Fredrickson, G. H. *Phys. Rev. Lett.* **1994**, *73*, 3235.
(57) Schmid, F.; Muller, M. *Macromolecules* **1995**, *28*, 8639.
(58) Chen, Z. Y. *Macromolecules* **1993**, *26*, 34193.
(59) Jiang, T.; Wu, J. Z. *J. Chem. Phys.* **2007**, *127*, 034902.